Supplemental data

Supplemental Figures

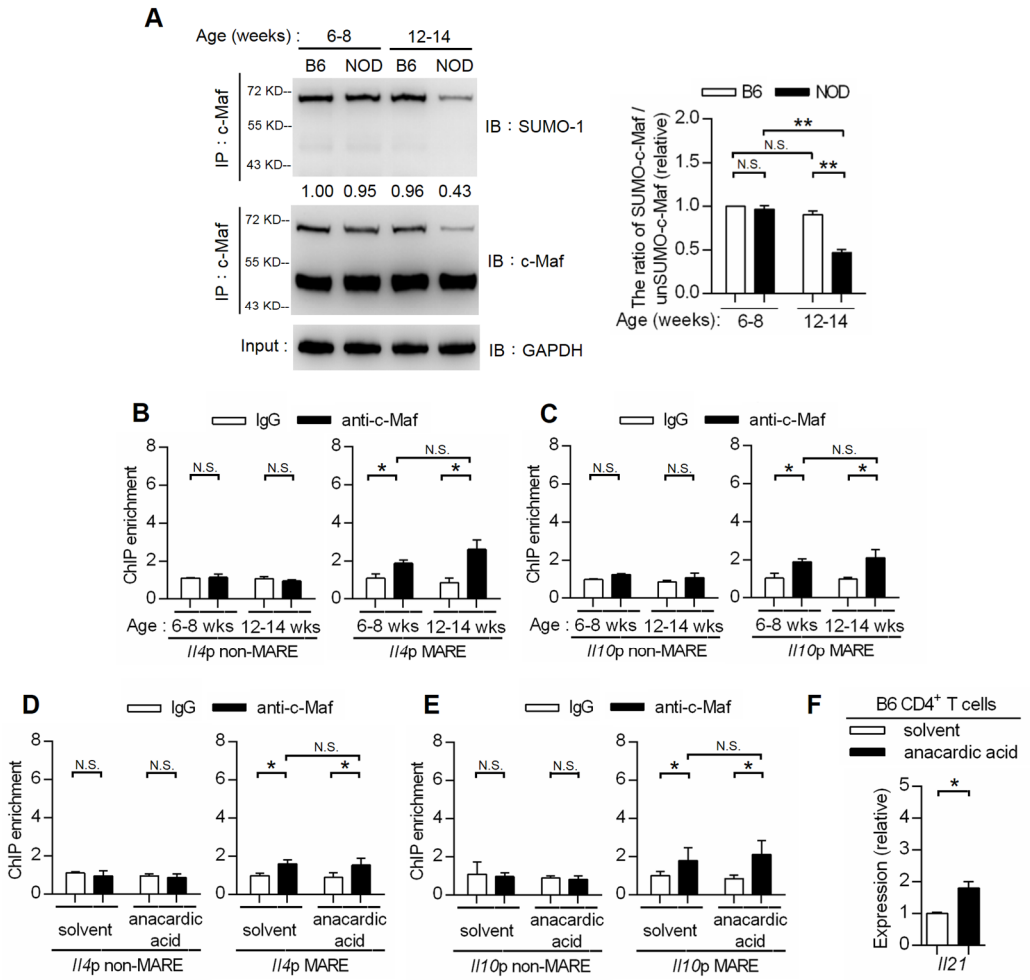

Supplemental Figure 1. (**A**) Immunoprecipitation analysis of c-Maf SUMOylation in 6–8- and 12–14-week-old B6 and NOD CD4$^+$ T cells cultured for 36 h with anti-CD3 and anti-CD28. (**B** and **C**) ChIP analysis of the interaction of c-Maf with the *Il4* promoter (**B**) or the *Il10* promoter (**C**) in 6–8- and 12–14-week-old NOD CD4$^+$ T cells cultured for 36 h with anti-CD3 and anti-CD28. Isotype-matched IgG was used as a control. (**D** and **E**) ChIP analysis of the interaction of c-Maf with the *Il4* promoter (**D**) or the *Il10* promoter (**E**) in CD4$^+$ T cells cultured for 36 h with anti-CD3 and anti-CD28 in the presence of anacardic acid (3 μM) or its solvent (DMSO), which were added after 18 h of culture. Isotype-matched IgG was used as a control. (**F**) Expression of *Il21* mRNA in B6 CD4$^+$ T cells cultured for 36 h with anti-CD3 and anti-CD28 in the presence of anacardic acid (3 μM) or its solvent (DMSO), which were added after 18 h of culture. Data represent the mean ± SEM. n = 5 mice (**A**) or n = 3 mice (**B**-**F**) per group. 3 independent experiments. *p < 0.05; **p < 0.01; N.S., not significant by one-way ANOVA with Tukey's post test (**A**-**E**) or 2-tailed Student's t test (**F**).

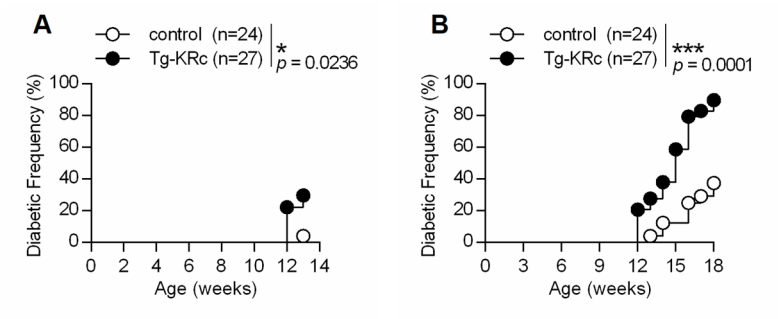

Supplemental Figure 2. (**A** and **B**) Diabetes incidence in Tg-KRc NOD mice and their littermate controls. *p < 0.05; ***p < 0.001 by log-rank test.

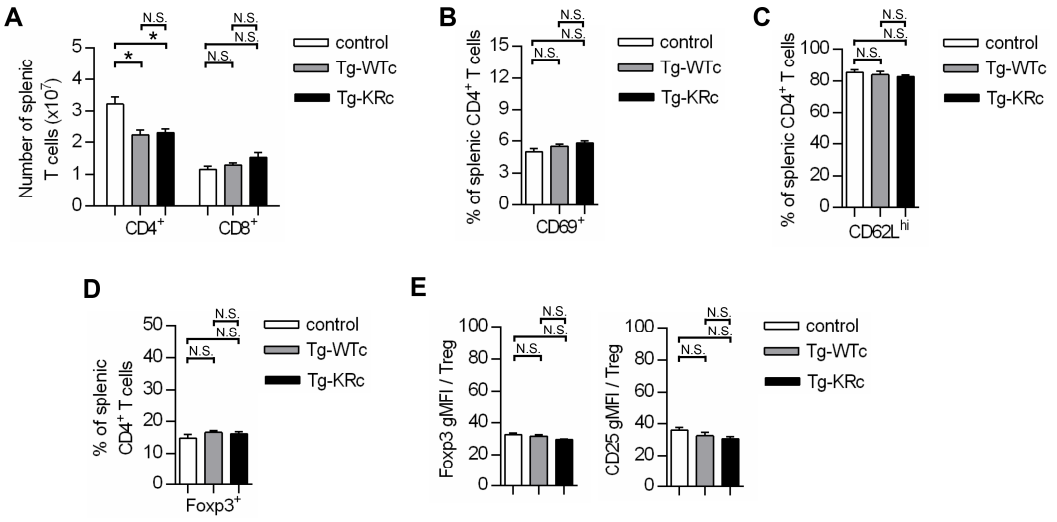

Supplemental Figure 3. (**A**) Summary of the number of splenic $CD4^+$ or $CD8^+$ T cells in 6–8-week-old control, Tg-WTc and Tg-KRc NOD mice. (**B**–**E**) Flow cytometry analysis of the expression of CD69 (**B**), CD62L (**C**), Foxp3 (**D** and **E**) or CD25 (**E**) in splenic $CD4^+$ T cells from 6–8-week-old control, Tg-WTc and Tg-KRc NOD mice. Summary of the frequency of $CD69^+CD4^+$ (**B**), $CD62L^{hi}CD4^+$ (**C**) or $Foxp3^+CD4^+$ (**D**) T cells. Summary of the geometric mean fluorescent intensity (gMFI) of Foxp3 (left panel in **E**) or CD25 (right panel in **E**) in $CD4^+$ T cells. Data represent the mean ± SEM. $n = 5$ mice per group. 3–4 independent experiments. $^*p < 0.05$; N.S., not significant by one-way ANOVA with Tukey's post test.

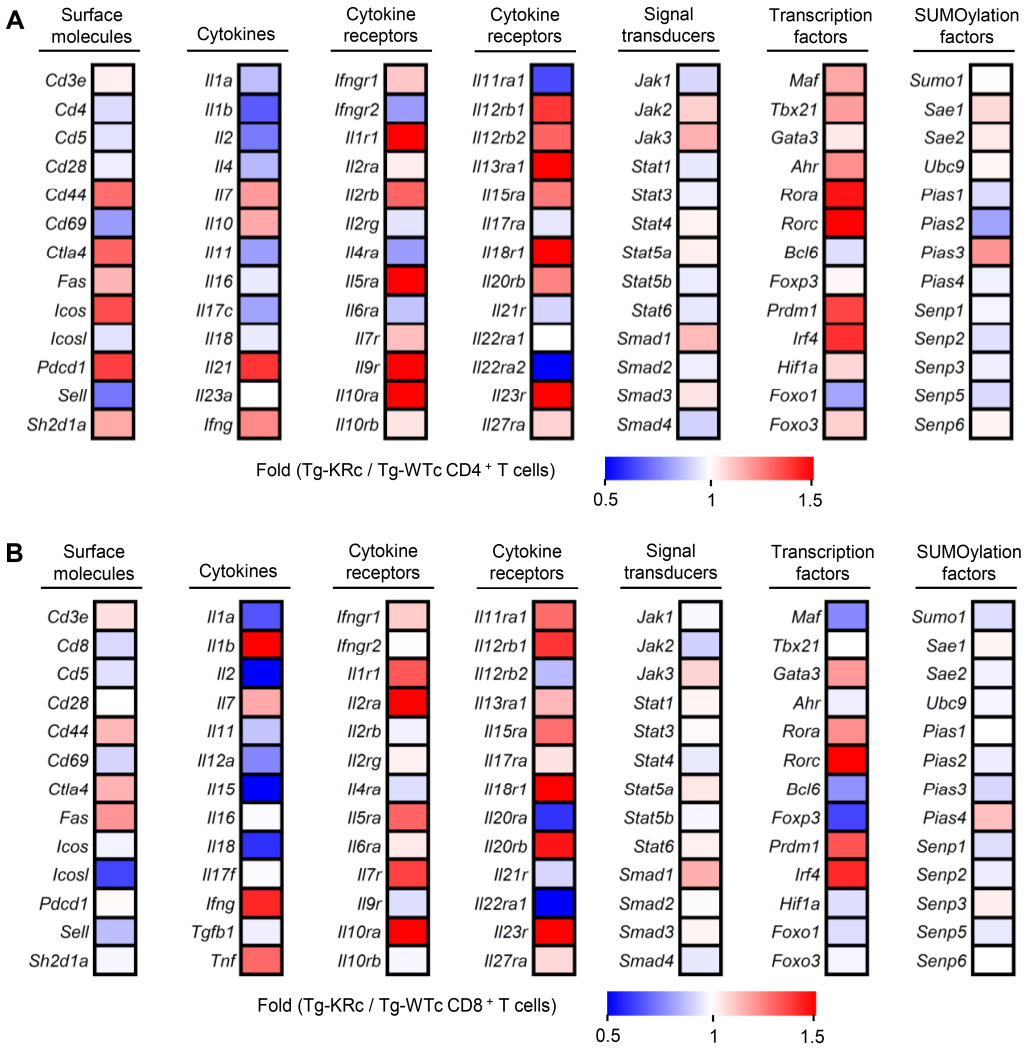

Supplemental Figure 4. (**A** and **B**) RNA-seq analysis of CD4$^+$ (**A**) or CD8$^+$ (**B**) T cells from 12–14-week-old Tg-WTc and Tg-KRc NOD mice (n = 3 mice per group). Heatmap of selected genes (fold change) that are differentially expressed between Tg-WTc cells and Tg-KRc cells. Colors indicate upregulated (red) and downregulated (blue) genes in Tg-KRc cells compared with Tg-WTc cells.

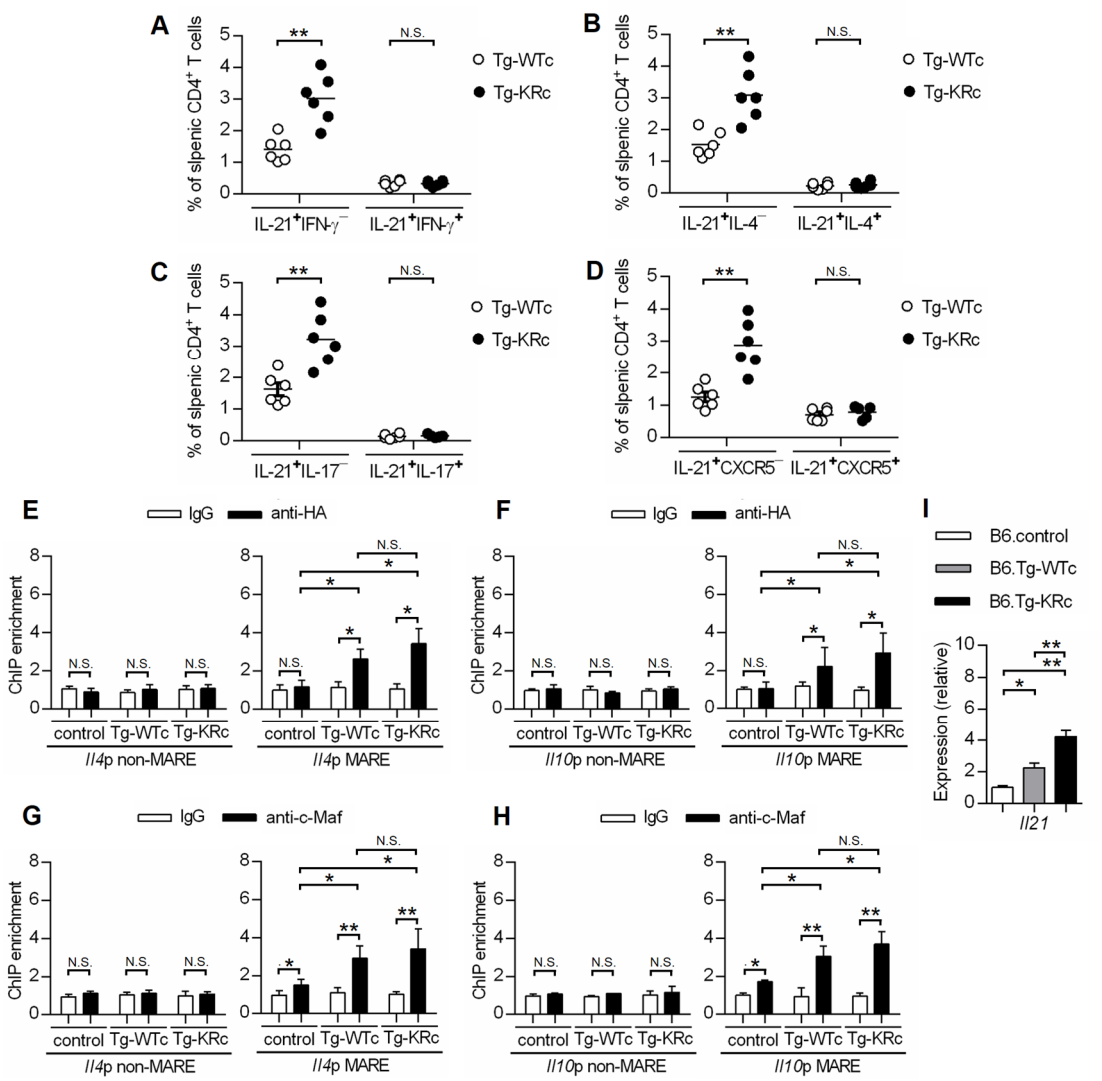

Supplemental Figure 5. (**A**–**D**) Flow cytometry analysis of the expression of IL-21, IFN-γ, IL-4, IL-17, and CXCR5 in splenic CD4$^+$ T cells from 12–14-week-old control, Tg-WTc and Tg-KRc NOD mice. Summary of the frequencies of IL-21$^+$IFN-γ$^-$ and IL-21$^+$IFN-γ$^+$ CD4$^+$ T cells (**A**), IL-21$^+$IL-4$^-$ and IL-21$^+$IL-4$^+$ CD4$^+$ T cells (**B**), IL-21$^+$IL-17$^-$ and IL-21$^+$IL-17$^+$ CD4$^+$ T cells (**C**), or IL-21$^+$CXCR5$^-$ and IL-21$^+$CXCR5$^+$ CD4$^+$ T cells (**D**). (**E**–**H**) ChIP analysis of the interaction of c-Maf with the *Il4* promoter (**E** and **G**) or the *Il10* promoter (**F** and **H**) in naïve control, Tg-WTc and Tg-KRc NOD CD4$^+$ T cells cultured for 36 h with anti-CD3 and anti-CD28. Isotype-matched IgG was used as a control. (**I**) Expression of *Il21* mRNA in naïve control, Tg-WTc and Tg-KRc B6 CD4$^+$ T cells cultured with anti-CD3 and anti-CD28 for 36 h. Data represent the mean ± SEM. n = 6 mice (**A**–**D**), n = 5 mice (**E-H**), n = 3 mice (**I**) per group. 3–4 independent experiments. *$p < 0.05$; **$p < 0.01$; N.S., not significant by 2-tailed Student's t test (**A**–**D**) or one-way ANOVA with Tukey's post test (**E**–**I**).

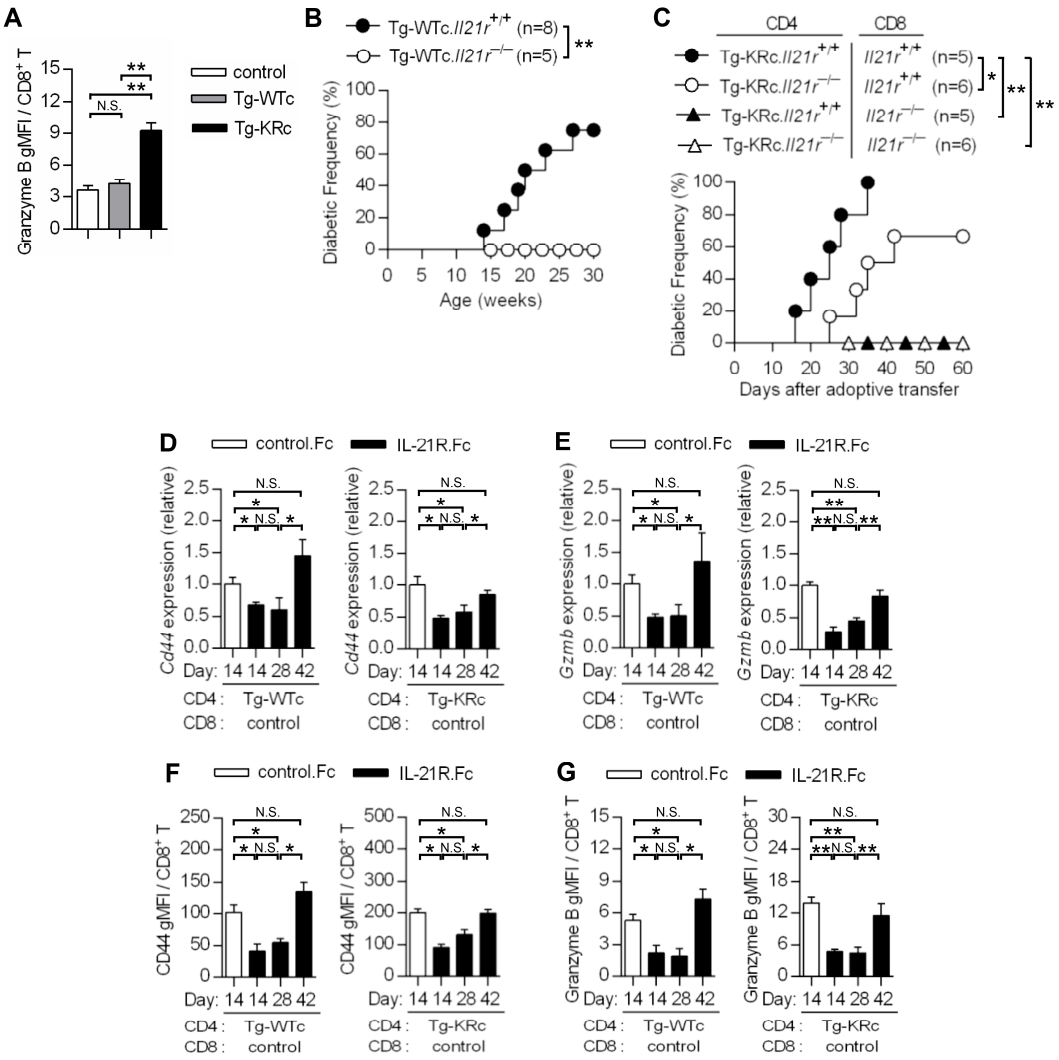

Supplemental Figure 6. (**A**) Flow cytometry analysis of the granzyme B expression in splenic CD8$^+$ T cells from 12–14-week-old control, Tg-WTc and Tg-KRc NOD mice. Summary of the geometric mean fluorescent intensity (gMFI) of granzyme B in CD8$^+$ T cells. (**B**) Diabetes incidence in Tg-WTc.*Il21r*$^{+/+}$ and Tg-WTc.*Il21r*$^{-/-}$ NOD mice. (**C**) Diabetes incidence in NOD.*Rag1*$^{-/-}$ recipients injected with CD25$^-$CD4$^+$ T cells from Tg-KRc.*Il21r*$^{+/+}$ or Tg-KRc.*Il21r*$^{-/-}$ NOD mice plus CD8$^+$ T cells from *Il21r*$^{+/+}$ or *Il21r*$^{-/-}$ NOD mice. (**D**–**G**) NOD.*Rag1*$^{-/-}$ recipients were injected with Tg-WTc and Tg-KRc CD25$^-$CD4$^+$ T cells plus control CD8$^+$ T cells on day 0, and then injected with control.Fc or IL-21R.Fc (10 μg) every 2 days from day 1 to day 13. RT–qPCR analysis of the expression of *Cd44* (**D**) or *Gzmb* (**E**) in CD8$^+$ T cells or Flow cytometry analysis of the expression of CD44 (**F**) or granzyme B (**G**) in CD8$^+$ T cells from NOD.*Rag1*$^{-/-}$ recipients on day 14, day 28 or day 42. Summary of the geometric mean fluorescent intensity (gMFI) of CD44 (**F**) or granzyme B (**G**) in CD8$^+$ T cells. Data represent the mean ± SEM. $n = 6$ mice (**A**) or $n = 3$ mice (**D**–**G**) per group. 3 independent experiments (**A**) or 2 independent experiments (**C**–**G**). *$p < 0.05$; **$p < 0.01$; N.S., not significant by one-way ANOVA with Tukey's post test (**A, D**–**G**) or log-rank test (**B** and **C**).

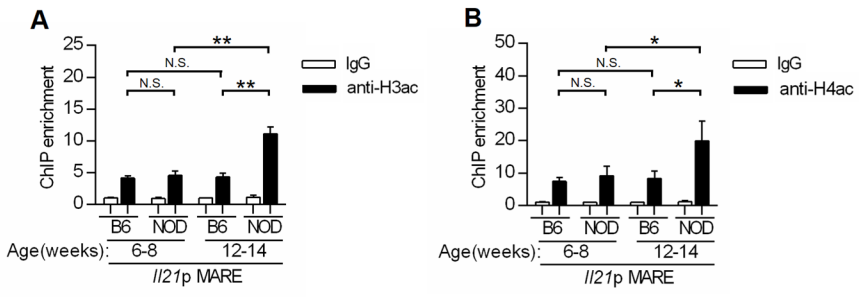

Supplemental Figure 7. (**A** and **B**) ChIP analysis of the abundance of H3ac (**A**) and H4ac (**B**) in the c-Maf-binding site of the *Il21* promoter in 6–8- and 12–14-week-old B6 and NOD $CD4^+$ T cells cultured for 36 h with anti-CD3 and anti-CD28. Isotype-matched IgG was used as a control. Data represent the mean ± SEM. n = 3 mice per group. 3 independent experiments. *p < 0.05; **p < 0.01; N.S., not significant by one-way ANOVA with Tukey's post test.

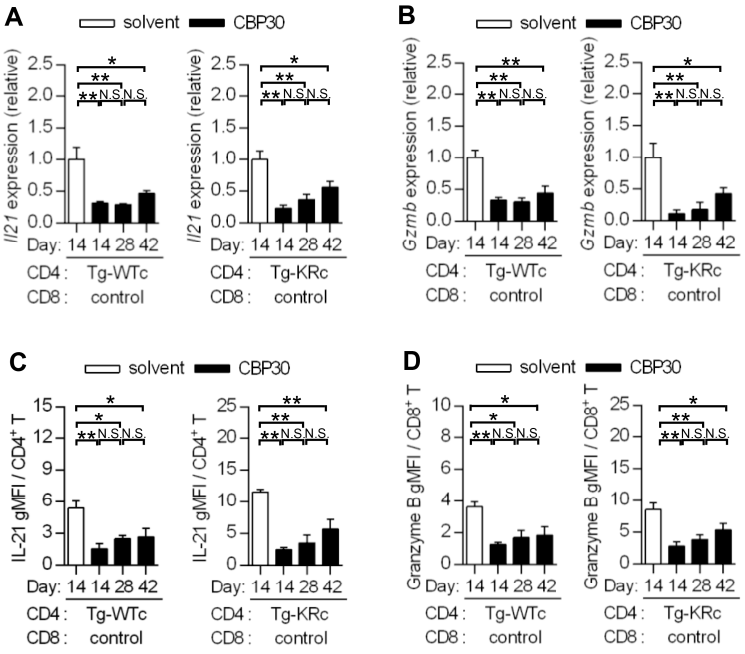

Supplemental Figure 8. (**A**–**D**) NOD.*Rag1*$^{-/-}$ recipients were injected with Tg-WTc or Tg-KRc CD25^{-}CD4^{+} T cells plus control CD8^{+} T cells on day 0, and then injected with 2 mg/kg CBP30 or its solvent (DMF) every 2 days from day 1 to day 13. RT–qPCR analysis of the expression of *Il21* in CD4^{+} T cells (**A**) and the expression of *Gzmb* in CD8^{+} T cells (**B**) or Flow cytometry analysis of the expression of IL-21 in CD4^{+} T cells (**C**) and the expression of granzyme B in CD8^{+} T cells (**D**) from NOD.*Rag1*$^{-/-}$ recipients on day 14, day 28 or day 42. Summary of the geometric mean fluorescent intensity (gMFI) of IL-21 in the CD4^{+} T cells (**C**) or granzyme B in the CD8^{+} T cells (**D**). Data represent the mean ± SEM. $n = 3$ mice per group. 2 independent experiments. *$p < 0.05$; **$p < 0.01$; N.S., not significant by one-way ANOVA with Tukey's post test.

Supplemental Methods

Reagents. PMA, ionomycin, monensin, anacardic acid and *N*-ethylmaleimide were purchased from Sigma-Aldrich. CBP30 (SGC-CBP30) was obtained from Cayman Chemical.

T cell purification and stimulation. $CD4^+$ T cells, $CD25^-CD4^+$ T cells, naïve $CD4^+$ T cells, $CXCR5^-ICOS^{lo}PD\text{-}1^{lo}CD4^+$ T cells, $CXCR5^-ICOS^{hi}PD\text{-}1^{hi}CD4^+$ T cells, $CXCR5^+ICOS^{hi}PD\text{-}1^{hi}CD4^+$ T cells and $CD8^+$ T cells were isolated from transgenic or nontransgenic NOD mice using a magnetic cell sorter autoMACS (Miltenyi Biotec) or a FACSAria cell sorter (BD Biosciences). The purity of isolated cells was >95%. Cells were stimulated with plate-coated anti-CD3 (5 μg/mL, 145-2C11/553058, BD Biosciences) plus soluble anti-CD28 (2 μg/mL, 37.51/102112, BioLegend) monoclonal antibodies for the indicated times.

Flow cytometric analysis. Cell suspensions of spleen cells and pancreatic infiltrating lymphocytes were prepared as previously described (1). For surface staining, cells were stained with fluorochrome-conjugated antibodies to CD4 (RM4-5/17-0042, eBioscience), CD8 (53-6.7/100712, BioLegend), CD44 (IM7/11-0441, eBioscience), CD69 (H1.2F3/104520, BioLegend), ICOS (C398.4A/313506, BioLegend), PD-1 (J43/12-9985, eBioscience), CXCR5 (L138D7/145508, BioLegend) and KLRG1 (2F1/12-5893, eBioscience). For intracellular cytokine staining, cells were stimulated for 4 h at 37 °C with PMA (20 ng/mL), ionomycin (1 μg/mL) and monensin (GolgiStop; 4 μM). After being stained for surface markers, cells were fixed, permeabilized and stained with fluorochrome-conjugated antibodies against IFN-γ (XMG1.2, eBioscience), IL-4 (11B11/504106, BioLegend), IL-10 (JES5-16E3/11-7101, eBioscience), IL-17A (TC11-18H10.1/506915, BioLegend) and granzyme B (NGZB/12-8898, eBioscience). For detection of IL-21, cells were incubated with recombinant IL-21R.Fc chimera (R&D Systems) and then stained with fluorochrome-conjugated anti-human IgG Fc antibody (HP6017/409304, BioLegend). Cells were analyzed by flow cytometry using a FACSCalibur (BD Biosciences).

Measurement of cytokines. IL-4, IL-10 and IL-21 secreted from T cells were measured in tissue culture supernatants using enzyme-linked immunosorbent assay (ELISA) kits (R&D Systems, Minneapolis, MN, USA) according to the manufacturer's instructions.

Reverse transcription–quantitative PCR. Total RNA was extracted using RNeasy mini kits (Qiagen) and used for cDNA synthesis using the SuperScript III synthesis kit (Invitrogen) according to the manufacturer's instructions. RT–qPCR was performed using the SYBR Green method. Expression was normalized to the expression of the housekeeping gene *Rps29*.

Immunoprecipitation and Western blot analysis. $CD4^+$ T cells were lysed using RIPA buffer (50 mM Tris, pH 7.4, 2% SDS, 150 mM NaCl) containing a protease inhibitor mixture (Sigma-Aldrich) on ice for 30 min. For detection of SUMO-conjugated c-Maf, $CD4^+$ T cells were washed twice with ice-cold PBS supplemented with 20 mM *N*-ethylmaleimide (NEM) and lysed in SDS lysis buffer (5% SDS, 0.15 M Tris-HCl pH 6.7 and 30% glycerol) diluted 1/2 in RIPA buffer containing protease inhibitor cocktail and 20 mM NEM (2). Cell debris was removed by centrifugation and the protein concentration in the supernatants was measured using the BCA Protein Assay kit (Thermo Fisher Scientific). For immunoprecipitation, total cell lysates were incubated with 2 μg of anti-HA (A190-108A, Bethyl Laboratories) or anti-c-Maf (M-153/sc-7866, Santa Cruz Biotechnology) overnight at 4 °C followed by incubation with 50 μL of protein G agarose (Millipore) for 2 h at 4 °C. Immunoprecipitates were washed five times with RIPA buffer and subjected to SDS–PAGE and Western blot analysis. After blotting, membranes were incubated overnight at 4 °C with anti-HA (3F10/11-867-423-001, Roche, Indianapolis, IN, USA), anti-c-Maf (M-153/sc-7866 or 6B8/sc-293420; Santa Cruz Biotechnology) or anti-SUMO-1 (D-11/sc-5308, Santa Cruz Biotechnology) antibodies and subsequently incubated with goat anti-rabbit HRP (Jackson ImmunoResearch Laboratories) or goat anti-rat light chain-HRP (Jackson ImmunoResearch Laboratories) for 1 h at room temperature. In some cases, blots were incubated with Clean-Blot IP detection reagent (Thermo Fisher Scientific). Protein signals were detected using

WesternBright ECL HRP substrate (Advansta Inc.) and visualized on a LAS-3000 imaging system (Fujifilm Life Science).

Adoptive transfer. $CD25^{-}CD4^{+}$ (4×10^6 cells) and $CD8^{+}$ (2×10^6 cells) T cells isolated from 12–14-week-old normoglycemic female NOD mice were transferred into 6–8-week-old female NOD.*Rag1*$^{-/-}$ mice. Urine glucose concentration in the recipients was measured daily. NOD.*Rag1*$^{-/-}$ recipients were defined as diabetic when glycosuria > 500 mg/dL on two consecutive tests.

Chromatin immunoprecipitation (ChIP) assay. DNA–protein complexes were cross-linked with 1% formaldehyde and lysed with SDS buffer (50 mM Tris-HCl, pH 8.1, 10 mM EDTA, 1% SDS and protease inhibitors). Lysates were sonicated and supernatants were collected after centrifugation. Lysates were diluted with ChIP dilution buffer (20 mM Tris-HCl, pH 8.1, 2 mM EDTA, 150 mM NaCl and 1% Triton X-100). Diluted lysates were incubated with 2 μg of antibodies overnight at 4 °C and then immunoprecipitated with protein A/G magnetic beads for another 2 h. The magnetic bead–antibody–chromatin complexes were then washed three times with RIPA buffer, followed by two washes with Tris-EDTA buffer. After elution using elution buffer (1% SDS and 0.1 M $NaHCO_3$), DNA–protein complexes were incubated at 65 °C overnight to reverse formaldehyde cross-linking. DNA fragments were recovered using a QIAquick DNA purification kit (Qiagen) and analyzed by qPCR with specific primers (Supplemental Table 5). The following antibodies were used for ChIP experiments: anti-HA (A190-108A, Bethyl Laboratories), anti-c-Maf (M-153/sc-7866, Santa Cruz Biotechnology), anti-Daxx (M-112/sc-7152, Santa Cruz Biotechnology), anti-HDAC1 (ab-7028, Abcam), anti-HDAC2 (ab-7029, Abcam), anti-acetylated H3 (06-599, Millipore), anti-acetylated H4 (06-866, Millipore), anti-CBP (D6C5/7389, Cell Signaling Technology) and anti-p300 (C-20/sc-585, Santa Cruz Biotechnology).

References

1. Yeh LT, Miaw SC, Lin MH, Chou FC, Shieh SJ, Chuang YP, Lin SH, Chang DM, and Sytwu HK. Different modulation of Ptpn22 in effector and regulatory T cells leads to attenuation of autoimmune diabetes in transgenic nonobese diabetic mice. *Journal of immunology.* 2013;191(2):594-607.
2. Leavenworth JW, Ma XJ, Mo YY, and Pauza ME. SUMO Conjugation Contributes to Immune Deviation in Nonobese Diabetic Mice by Suppressing c-Maf Transactivation of IL-4. *Journal of immunology.* 2009;183(2):1110-9.

Supplemental Table 1

A

Age (weeks):	6-8	12-14
intensity of SUMO-c-Maf :	7920	3080
intensity of unSUMO-c-Maf :	25517	27360
$\frac{\text{SUMO-c-Maf}}{\text{unSUMO-c-Maf}}$ ratio :	0.310	0.113
normalized ratio	1.00	0.36

B

Age (weeks):	6-8		12-14	
	B6	NOD	B6	NOD
intensity of SUMO-c-Maf :	8894	9138	9276	3574
intensity of unSUMO-c-Maf :	18111	19491	19663	17024
$\frac{\text{SUMO-c-Maf}}{\text{unSUMO-c-Maf}}$ ratio :	0.491	0.469	0.472	0.210
normalized ratio	1.00	0.95	0.96	0.43

C

	solvent	anacardic acid
intensity of SUMO-c-Maf :	8261	3541
intensity of unSUMO-c-Maf :	20791	18090
$\frac{\text{SUMO-c-Maf}}{\text{unSUMO-c-Maf}}$ ratio :	0.397	0.196
normalized ratio :	1.00	0.49

Supplemental Table 2

	control	Tg-WTc	Tg-KRc
intensity of SUMO-c-Maf :	4899	11579	5255
intensity of unSUMO-c-Maf :	11438	25769	24738
$\frac{\text{SUMO-c-Maf}}{\text{unSUMO-c-Maf}}$ ratio :	0.428	0.449	0.212
normalized ratio	1.00	1.05	0.50

Supplemental Table 3

CD4	CD8	Treatment	Diabetic onset of each recipient (days)
Tg-WTc	control	control.Fc	25 32 38 42
Tg-KRc	control	control.Fc	16 18 20 22 25
Tg-WTc	control	IL-21R.Fc	35 45 52 55 60
Tg-KRc	control	IL-21R.Fc	40 42 46 50 55

Supplemental Table 4

CD4	CD8	Treatment	Diabetic onset of each recipient (days)
Tg-WTc	control	solvent	25 28 28 32 38
Tg-KRc	control	solvent	15 16 18 20 23
Tg-WTc	control	CBP30	42 55 60
Tg-KRc	control	CBP30	40 42 48 55

Supplemental Table 5: Primer for the ChIP assay

Promoter region		Sequence (5' to 3')
*Il4*p non-MARE	F	TTCACCCAAAGAGAGCTCAG
	R	TGTTCTGTAGGCCTAGGGAC
*Il4*p MARE	F	GTGGCAACCCTACGCTGATAAG
	R	GCTAACAATGCAATGCTGGCAG
*Il10*p non-MARE	F	CAGTCAGGAGAGAGGGCAGTGA
	R	TTTCCAACAGCAGAAGCAAC
*Il10*p MARE	F	CTCTCCTCTGACCAACTGCC
	R	TGGGTTGAACGTCCGATATT
*Il21*p non-MARE	F	TACACTACGGTCCATAACAG
	R	ATCCCCAAAGCAGTGGTTCTC
*Il21*p MARE	F	TGGTGAATGCTGAAAACTGGAA
	R	CCCATCTGCATCTTAGACAGGAA

Figure 1A

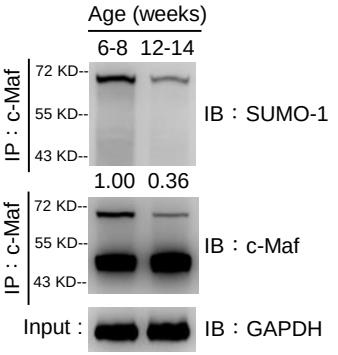
Age (weeks)
6-8 12-14
IP：c-Maf
72 KD--
55 KD--
43 KD--
IB：SUMO-1
1.00 0.36
IP：c-Maf
72 KD--
55 KD--
43 KD--
IB：c-Maf
Input：
IB：GAPDH

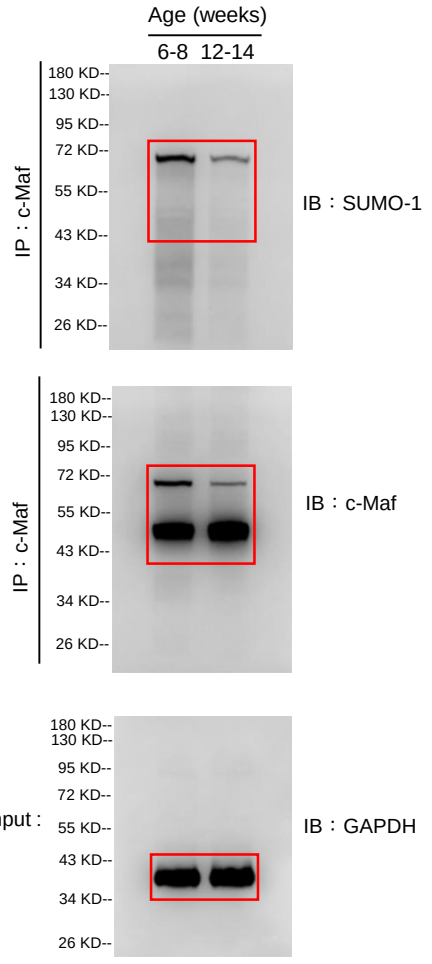
Age (weeks)
6-8 12-14
IP：c-Maf
180 KD--
130 KD--
95 KD--
72 KD--
55 KD--
43 KD--
34 KD--
26 KD--
IB：SUMO-1
IP：c-Maf
IB：c-Maf
Input：
IB：GAPDH

Figure 1F

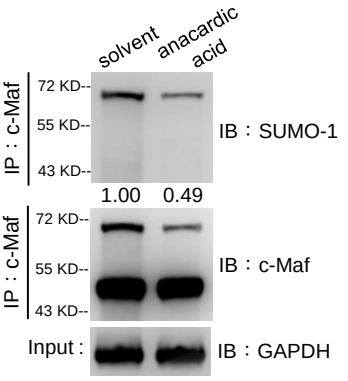
solvent
anacardic acid
IP：c-Maf
72 KD--
55 KD--
43 KD--
IB：SUMO-1
1.00
0.49
IP：c-Maf
72 KD--
55 KD--
43 KD--
IB：c-Maf
Input :
IB：GAPDH

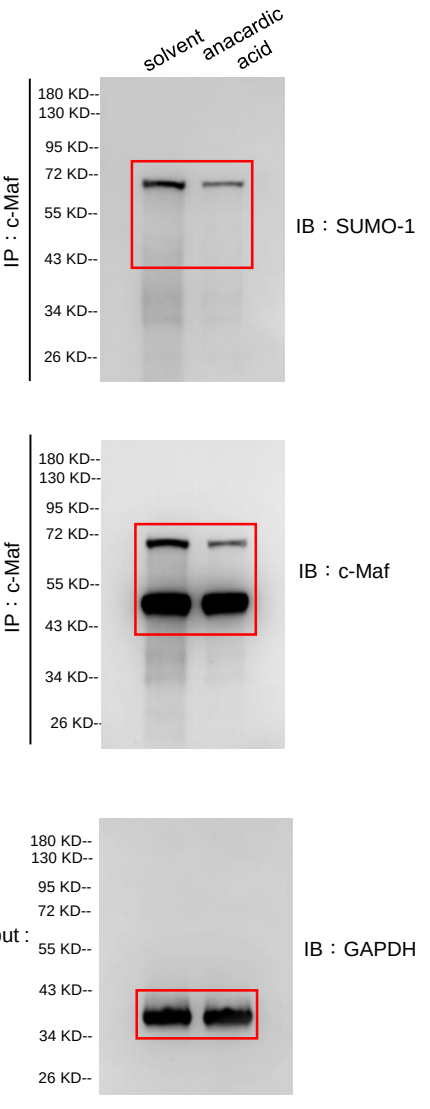
solvent
anacardic acid
IP：c-Maf
180 KD--
130 KD--
95 KD--
72 KD--
55 KD--
43 KD--
34 KD--
26 KD--
IB：SUMO-1
IP：c-Maf
IB：c-Maf
Input :
IB：GAPDH

Figure 2B

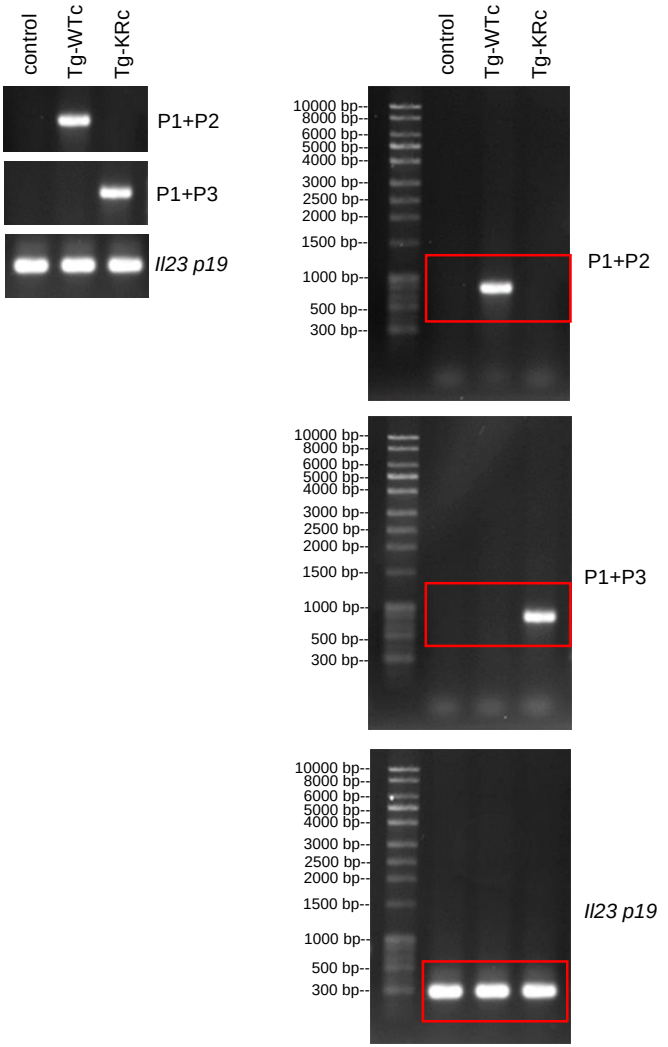
control
Tg-WTc
Tg-KRc
P1+P2
P1+P3
Il23 p19
10000 bp--
8000 bp--
6000 bp--
5000 bp--
4000 bp--
3000 bp--
2500 bp--
2000 bp--
1500 bp--
1000 bp--
500 bp--
300 bp--

Figure 2C

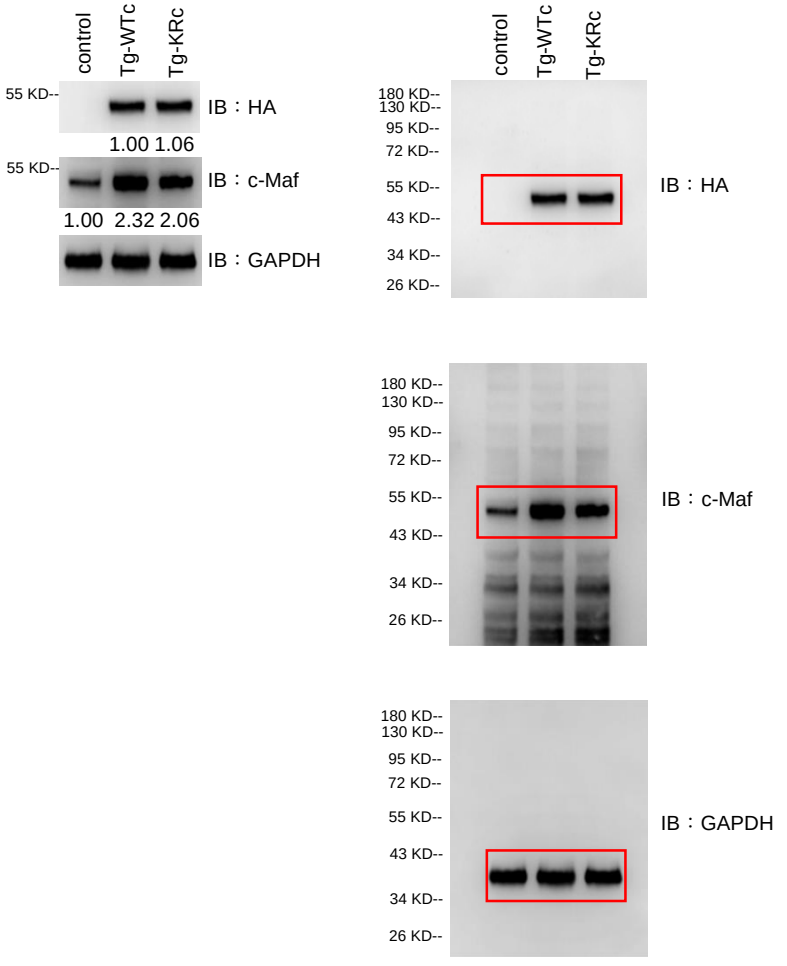
control
Tg-WTc
Tg-KRc
55 KD--
IB：HA
1.00 1.06
55 KD--
IB：c-Maf
1.00 2.32 2.06
IB：GAPDH
180 KD--
130 KD--
95 KD--
72 KD--
55 KD--
43 KD--
34 KD--
26 KD--
IB：HA
IB：c-Maf
IB：GAPDH

Figure 2D

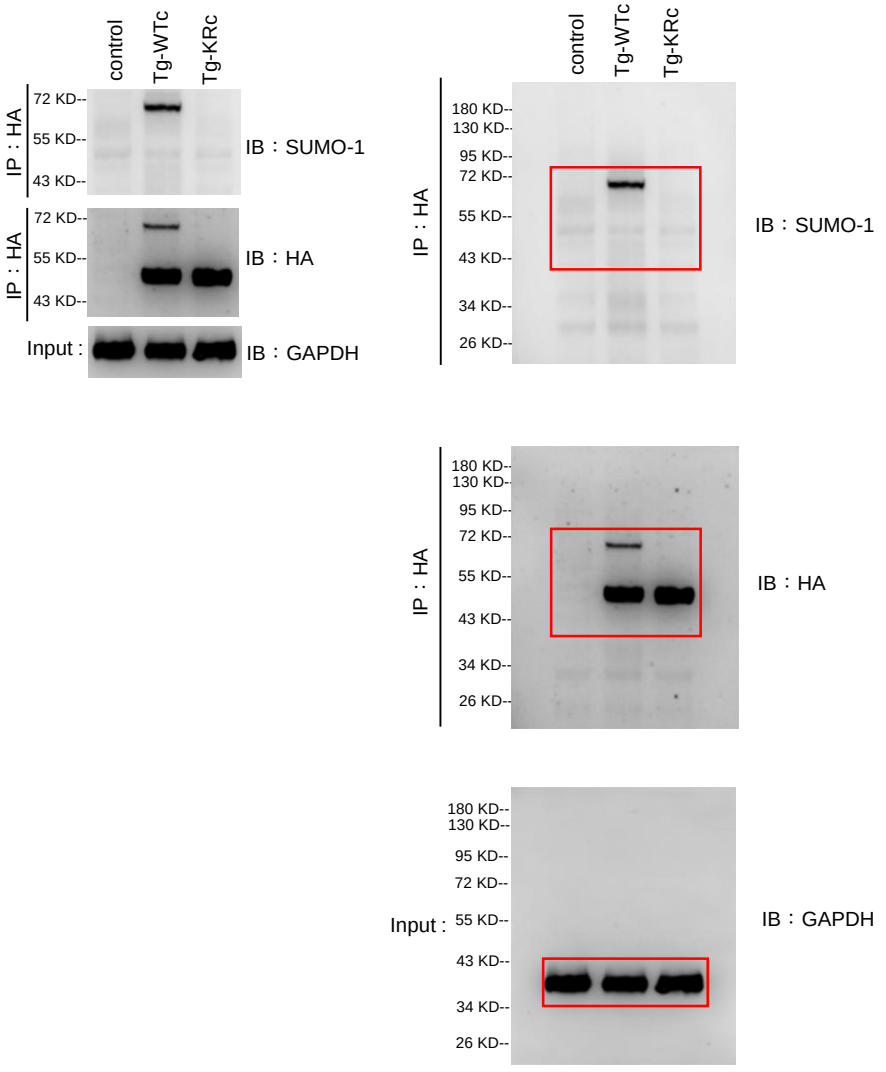
control
Tg-WTc
Tg-KRc
IP : HA
72 KD--
55 KD--
43 KD--
IB : SUMO-1
IP : HA
72 KD--
55 KD--
43 KD--
IB : HA
Input :
IB : GAPDH
control
Tg-WTc
Tg-KRc
IP : HA
180 KD--
130 KD--
95 KD--
72 KD--
55 KD--
43 KD--
34 KD--
26 KD--
IB : SUMO-1
IP : HA
180 KD--
130 KD--
95 KD--
72 KD--
55 KD--
43 KD--
34 KD--
26 KD--
IB : HA
Input :
180 KD--
130 KD--
95 KD--
72 KD--
55 KD--
43 KD--
34 KD--
26 KD--
IB : GAPDH

Figure 2E

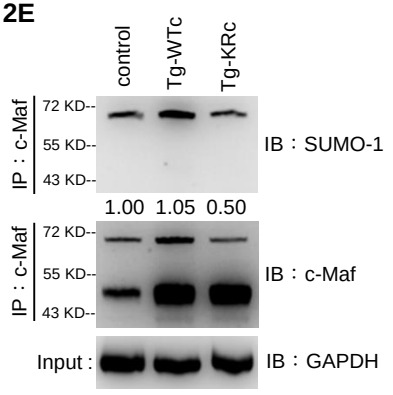
control
Tg-WTc
Tg-KRc
IP : c-Maf
72 KD--
55 KD--
43 KD--
IB : SUMO-1
1.00 1.05 0.50
IP : c-Maf
72 KD--
55 KD--
43 KD--
IB : c-Maf
Input :
IB : GAPDH

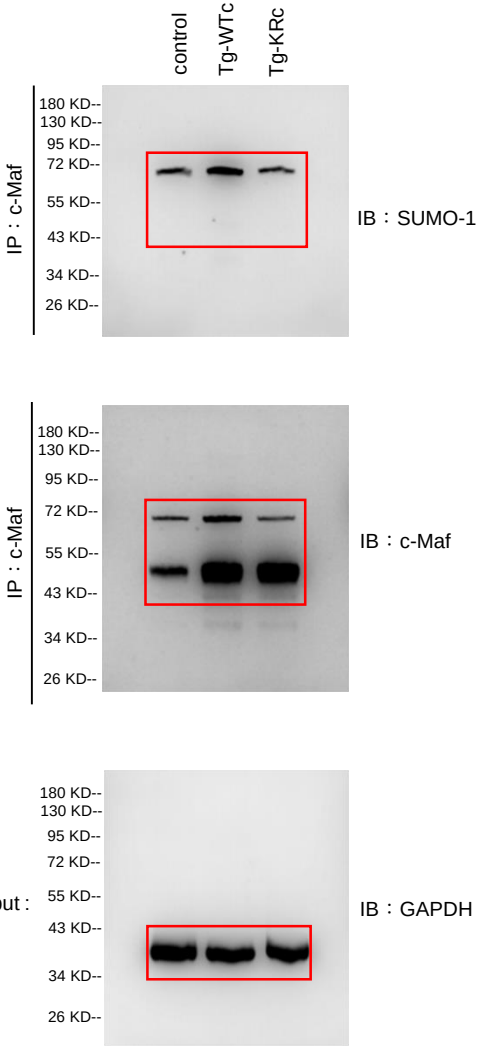
control
Tg-WTc
Tg-KRc
IP : c-Maf
180 KD--
130 KD--
95 KD--
72 KD--
55 KD--
43 KD--
34 KD--
26 KD--
IB : SUMO-1
IP : c-Maf
IB : c-Maf
Input :
IB : GAPDH

Supplemental Figure 1A